

# Fabrication and Testing of 18-mm-Period, 0.5-m-Long Nb<sub>3</sub>Sn Superconducting Undulator

I. Kesgin, M. Kasa, S. MacDonald, Y. Ivanyushenkov, E. Barzi, D. Turrioni, D. Arbelaez, Q. Hasse, A.V. Zlobin, S. Prestemon, and E. Gluskin

**Abstract**— The Advanced Photon Source at Argonne National Laboratory, in collaboration with FNAL and LBNL, is developing a Nb<sub>3</sub>Sn superconducting undulator with the goal of installing this device on the APS storage ring. A series of short, ~ 8-cm-long, 18-mm-period undulator prototype magnets have been designed, fabricated, and tested. The same design was scaled to fabricate a 0.5-m-long undulator prototype. Tests of this prototype showed that the designed peak magnetic field of 1.2 T at 850 A was successfully achieved. It represents at least a 20% improvement in comparison with a NbTi SCU having the same period and magnetic gap. Test results and lessons learned from the design process are reported.

**Index Terms**—Nb<sub>3</sub>Sn, superconducting undulator, SCU, stability, magnet design, quench

## I. INTRODUCTION

THE superconducting undulator (SCU) team at the Advanced Photon Source, in collaboration with Fermilab and LBNL, has been working on the design and fabrication of a new Nb<sub>3</sub>Sn-based SCU. A spatially periodic magnetic field generated by a pair of undulator magnets induces an oscillatory motion of relativistic electrons, which results in the emission of high-energy x-ray photons. The main goals of this project are to advance Nb<sub>3</sub>Sn-based SCU technology, and to deliver a novel x-ray source to APS users. A new, ~1.1-m-long, 1.8-cm-period Nb<sub>3</sub>Sn SCU will replace the existing NbTi SCU and, since the new device is almost the same length as the existing one, the brightness of the x-rays will be preserved but the spectral range will be extended.

Several attempts in the last decade to introduce Nb<sub>3</sub>Sn SC material into undulator technology did not bring to life any device that could be used at the light source [1-6]. These attempts highlighted significant technical challenges in the path toward building a Nb<sub>3</sub>Sn SCU that meets the requirements of existing light sources. Recognizing these challenges and capitalizing on the successful APS experience with NbTi SCUs, the project was divided into three phases. In Phase I, a series of short,

~ 8-cm-long, 18-mm-period undulator prototype magnets were fabricated, and, from one prototype to the next, the design was iteratively optimized [7, 8]. In Phase II, the main effort was focused on scaling the short magnet design to an intermediate length of about 0.5 m. The main motivation for this intermediate exercise was to optimize the insulation between the wire and magnet winding former and to develop a robust quench detection and protection system. Several new insulation schemes were investigated. The final choice of insulation scheme and optimized quench protection system will ensure the reliable operation of the SCU and its robust defense against the high voltages generated during a quench. In Phase III, full-length magnets, ~ 1.1 m long, will be designed, fabricated, and tested. In the final phase of the project, a novel Nb<sub>3</sub>Sn SCU will be installed on the APS storage ring to provide bright x-ray beam to the APS users.

In parallel with building the Nb<sub>3</sub>Sn SCU magnets, modifications of the existing cryostat are ongoing. These modifications were primarily triggered by the high operating current of the Nb<sub>3</sub>Sn SCU, which almost doubles the maximum operating current of NbTi SCUs. The magnet cooling approach for the Nb<sub>3</sub>Sn SCU duplicates the well-proven cooling scheme of the NbTi SCU [9, 10].

Currently, both Phases I and II of the project have been completed. The design of the short undulator prototype is scaled up to an intermediate (~ 0.5 m) length, and details of the test results are presented in the following sections.

## II. Nb<sub>3</sub>SN SUPERCONDUCTING UNDULATOR DESIGN OPTIMIZATIONS AND FABRICATION

The design approach for the magnet follows the footsteps of the NbTi SCU magnets [9, 11, 12]. In short, each of two SCU magnets consists of the magnet former made of a soft iron. Each magnet former has a multitude of grooves on its body to accommodate the SC wire [13]. The magnet parameters are provided in Table I. For comparison, the table also gives the parameters of the NbTi-based SCU currently operating at the APS. Design optimizations are highlighted below.

### A. Magnet Design

The Nb<sub>3</sub>Sn magnet design was iteratively optimized using short undulator prototypes. Several of these optimizations led to the design of the short undulator prototypes that met the desired SCU performance level [7].

Manuscript received on November 10, 2020. This work was supported by the U.S. Department of Energy, Office of Science, under Contract DE-ACO2-O6CH11357. (Corresponding author: Ibrahim Kesgin)

I. Kesgin, M. Kasa, S. MacDonald, Y. Ivanyushenkov, Q. Hasse, and E. Gluskin are with Advanced Photon Source, Argonne National Laboratory, Lemont, IL 60439 USA (e-mail: [ikesgin@anl.gov](mailto:ikesgin@anl.gov)).

E. Barzi, D. Turrioni, and A. V. Zlobin are with Fermilab, Batavia, IL 60510 USA.

D. Arbelaez and S. Prestemon are with Lawrence Berkeley National Laboratory, Berkeley, CA 94720 USA.

TABLE I  
 Nb<sub>3</sub>Sn SCU SPECIFICATIONS AND COMPARISONS WITH AN EXISTING  
 NbTi SCU

	Intermediate length Nb <sub>3</sub> Sn (IMM), 0.5m	NbTi SCU, 1.1m
Design Maximum undulator field (T)	1.2	0.97
Design maximum current ~80% of I <sub>c</sub> (A)	850	450
Magnetic gap (mm)	9.5	9.5
Number of turns in a coil pack	46	53
Number of periods	28.5	59.5
Groove width (mm)	5.35	5.25
Groove depth (mm)	4.9	4.2
Superconductor	Nb <sub>3</sub> Sn RRP 144/169*	NbTi 57 filament*
Wire diameter (mm)	0.6	0.6
Insulation thickness (~μm)	65	20

\*Nb<sub>3</sub>Sn and NbTi wires purchased from Bruker-OST and Supercon, respectively.

Magnetic simulations have been conducted to optimize the groove dimensions, and an ideal winding configuration was chosen for the best performance and convenient winding. Results of magnetic simulations were used as an input into mechanical simulations.

Mechanical simulations have been performed to calculate the deformation of the SCU magnets under high magnetic forces. It has been found that the forces at each end of the magnet are not counteracted due to the lack of neighboring winding. Simulations revealed large deformations in these areas, and the very

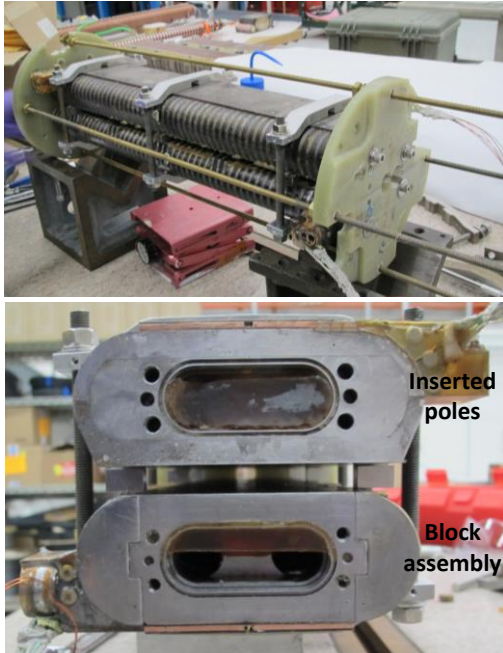


Fig 1. Photographs of the fabricated undulator magnets and assembly in the undulator configuration. Side view is shown at the bottom.

first short magnet design was optimized to reduce these deformations [7]. After several more iterations in the mechanical design of the former, the final design was initially chosen for scaling to an intermediate length of 0.5 m. This magnet design had inserted poles (Fig. 1, bottom). Basically, grooves in the magnet former were machined, pole pieces were inserted into these grooves, and the poles were secured with spring pins. Mechanical simulations addressed the pin positions to reduce the large deformations at the ends. The heat treatment cycle was also optimized during the short prototype studies [1, 14].

### B. 0.5-m-Long Undulator Fabrication

The design was further optimized to improve the mechanical robustness. Each magnet former was fabricated from multiple pieces, instead of inserted poles, and these pieces were bolted together from the sides. This is called a block assembly and is shown in Fig. 1, bottom. This design significantly improved the mechanical rigidity. Each groove on the assembled former was formed by slots machined in each separate piece. A 100-μm-thick mica layer was placed inside each groove prior to the winding, covering both bottom and sides of the grooves in both magnets, called IMM1 and IMM2. After winding was completed, the magnets were heat treated at the Technical Division facilities at FNAL.

After the heat treatments, the magnets were vacuum epoxy impregnated using CTD-101k epoxy and then cured in the furnace. Next each magnet, one after another, was quench-trained in a liquid helium (LHe) bath cryostat. After the training, the magnets were assembled as an undulator as shown in Fig. 1.

## III. RESULTS AND DISCUSSIONS

### A. Individual Magnet Training

Before the magnets were assembled into the undulator configuration, each magnet was trained in a LHe bath cryostat. The maximum training current was about 1000 A for both magnets. The IMM1 was cooled down twice; both training profiles are shown in Fig. 2a. The magnet demonstrated an excellent training memory after thermal cycling, and it required only one quench to reach the design current of 850 A. The training profile of IMM2 is shown in Fig 2b. It displayed similar behavior as IMM1, and only a few quenches were required to reach the design current.

### B. Quench Analysis

The operational current of a Nb<sub>3</sub>Sn undulator is almost twice as high as a NbTi undulator and thus requires a robust and reliable quench detection and protection system. An active protection scheme was implemented with an external dump resistor (0.25 Ohm for single-magnet tests) to extract the energy from the Nb<sub>3</sub>Sn undulator magnets. The expected maximum voltage level was 250 V at 1000 A, and the maximum coil-to-ground voltage the magnet can withstand was experimentally found in the short-magnet studies to be 500 V without breakdown. It

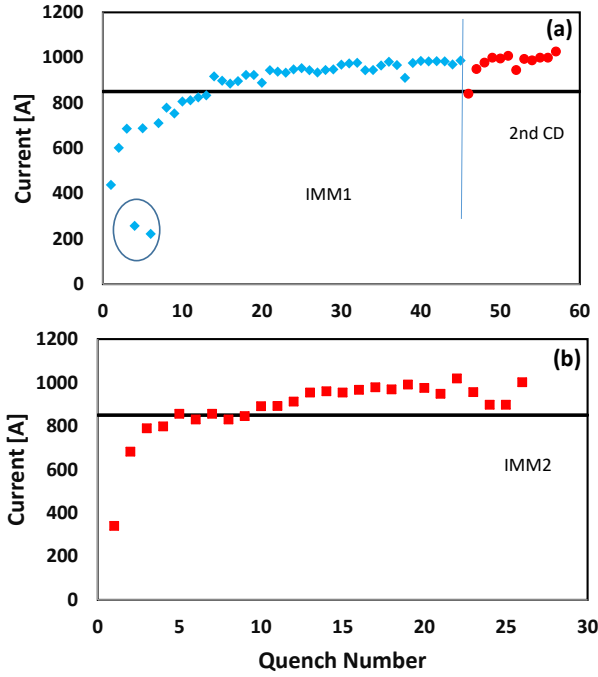


Fig 2. Training profiles for IMM1 (a) and IMM2 (b). The magnets required only a few quenches to reach the design current. The two quenches circled in the top plot are most likely false and triggered by the low set threshold voltage.

started showing some degradation when the magnet was exposed to 600-V terminal voltage attained by changing the dump resistor value and the quench current. A mica insulation layer between the Nb<sub>3</sub>Sn strands and the metallic former was introduced to improve this level in the 0.5-m-long magnets.

During a quench a hot spot forms, and the hot spot temperature can be calculated, assuming an adiabatic system, by integrating the  $I^2$  over the time span and using the temperature-dependent material properties. The hot spot temperatures calculated by this method are very conservative, and the real temperature is lower than the calculated ones.

The calculated hot spot temperatures are shown in Fig. 3 for current decaying from different current levels. The same calculations were performed including a 2-ms detection time. Typical detection time is lower than 1 ms. These temperature levels are significantly lower than the safe limit of 300 K [15], which indicate that there is still room to further adjust the dump resistor to reduce the maximum voltage that appears during a quench. It is important to note that all of these quenches are artificial, meaning that the current is kept at a certain value until the quench detection is manually triggered. The natural quench is triggered by a voltage drop caused by a hot spot formed due to a small disturbance that exceeds the minimum quench energy. The relevant voltage drop activates the detection system.

A center voltage tab is added in the magnet fabrications to measure the voltages from each half of the magnet, and the differential voltages are compared to a set threshold to detect the quench. Voltage profiles and current decay from 900 A during an artificial quench are shown in Fig. 4. The sum of the voltages from both halves of the magnet and the voltage across the resistor agree quite well. The temperature growth is also provided in

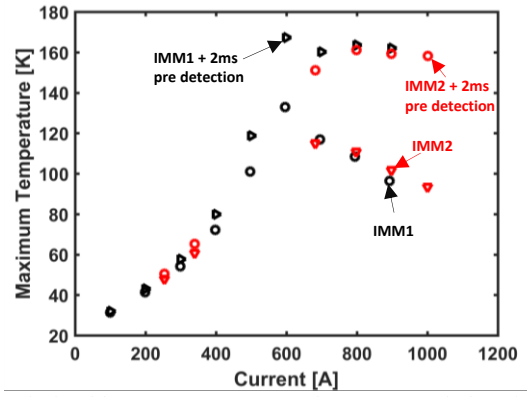


Fig. 3. Calculated hot spot temperatures. The 2-ms quench detection time is included in the calculation of the hot spot temperature along with the temperatures calculated in the cases of instant detections.

the same figure along with the current decay profile. Voltages from each half of the magnet slightly deviate when the dynamic losses start building the internal resistance. This effect starts earlier in the top half.

### C. 0.5-m-Long Undulator Assembly and Tests

Once the characterizations of the individual magnets were completed, both magnets were assembled into an undulator configuration with a magnetic gap of 9.5 mm—the same gap that is set for all APS planar NbTi undulators—and cooled down to LHe temperature (4.2 K). A 500-mOhm dump resistor that doubles the single magnet value was used in these tests. As standard practice, the excitation current was increased in increments of 100 A, at each step an intentional quench was initiated, and stored energy was extracted through the quench protection system. This was to make sure the magnets behaved as expected. The first intentional quench was at 100 A, and from the current and voltage profiles, it was confirmed that the time decay constant was the same as the single magnets. After charging the magnets to 700 A and initiating an intentional quench, both undulator magnets exhibited insulation breakdown. Analysis of the data showed that the most likely cause of the failure was due to weak locally specific ground insulation damage. This weakness was due to the relatively low quality of machining the

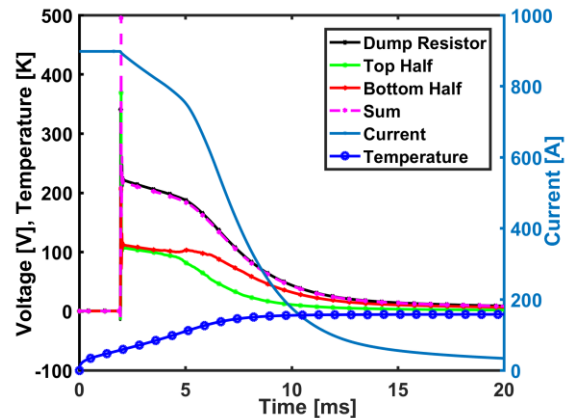


Fig 4. Voltages during an artificially induced quench from 900 A with a 250-m $\Omega$  dump resistor. Temperature growth and current decay with time are also shown.

grooves that house the coil windings in one of the magnets. In addition, it was found that fast opening IGBTs also induce a large voltage to the system, which could contribute to the failure.

#### D. Design Improvements and Second Set of 0.5-m-Long Undulator Magnets

Lessons learned from testing the first 0.5-m-long undulator prototype have been applied to the design and fabrication of the second 0.5-m-long prototype. The insulation on the second 0.5-m-long undulator prototype included a 100- $\mu\text{m}$ -thick plasma sprayed  $\text{Al}_2\text{O}_3$  layer in addition to a 100- $\mu\text{m}$ -thick mica layer. This brought the estimated safe voltage level to about 2-2.5 kV. The quench detection and protection system was also improved to significantly reduce the voltage spikes when the IGBTs opened. After implementing these design and hardware changes, a second set of 0.5-m-long undulator magnets were successfully tested.

IMM3 and IMM4 were individually trained, and the results are shown in Fig. 5. They are quite similar to the results obtained with the first set of magnets and required only a few quenches to reach the design current. Training results of two short undulator magnet prototypes are shown in the same figure. SMM3 represents the best short prototype and SMM6 – the worst. The 0.5-m-long prototype is about  $6\times$  longer than the short magnet prototype. However, the number of quenches required to reach the design current for the 0.5-m-long prototype was either the same or  $3\times$  the number of the short models and did not scale with the length. It is important to note that these current levels are 75-80% of the short sample limits, and it will require many more quench trainings to reach higher currents.

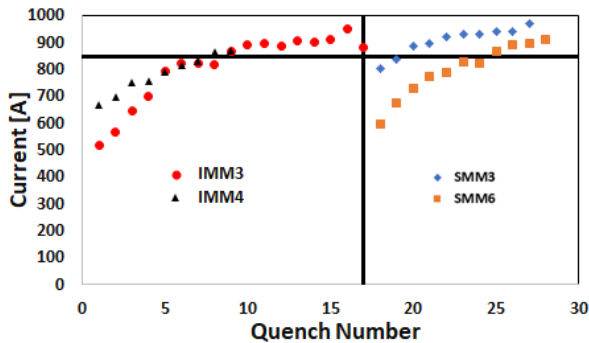


Fig. 5. Quench training profiles for 0.5-m-long magnets IMM3 & IMM4 (left) and comparisons with the  $\sim 8$ -cm-long short magnets SMM3 & SMM6 (right).

Right after the magnets reached the design current, the training was stopped, and the magnets were assembled into an undulator configuration to measure the field profiles and cool them down to LHe temperature. The magnets required only one quench to reach the maximum operating current of 850 A, which again indicates an excellent quench training memory. Then, the field profiles were measured every 100 A. The 0.5-m-long SCU structure delivered the design field of 1.2 T at around 850 A. A plot that compares the currently operating

NbTi-based SCU to the  $\text{Nb}_3\text{Sn}$ -based SCU is shown in Fig. 6. It is clear that the  $\text{Nb}_3\text{Sn}$  SCU provides at least 20% more field than its NbTi version.

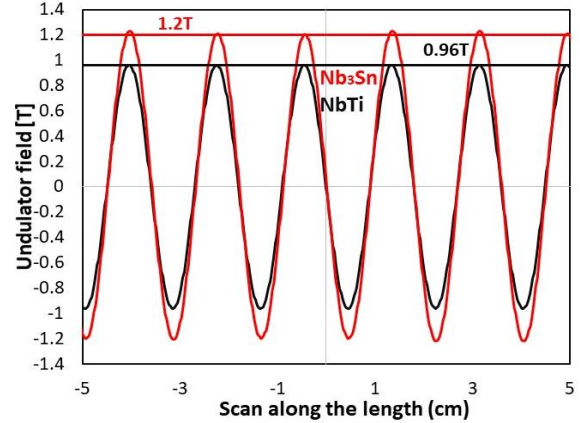


Fig 6. Field scans of a 0.5-m-long  $\text{Nb}_3\text{Sn}$  SCU and the 1.1-m-long currently operating NbTi SCU. The  $\text{Nb}_3\text{Sn}$  SCU provides at least a 20% increase in the undulator field.

#### IV. CONCLUSION

A 0.5-m-long  $\text{Nb}_3\text{Sn}$  SCU prototype undulator has been fabricated and successfully tested. The design peak field of 1.2 T at the maximum operating current of 850 A has been confirmed by the magnetic measurements. Further quench tests and analysis are ongoing to define the safe operation margin of the device. The design and fabrication of a 1.1-m-long  $\text{Nb}_3\text{Sn}$  SCU is currently in progress. The existing cryostat is being modified to accommodate the 1.1-m long  $\text{Nb}_3\text{Sn}$  SCU. The fully assembled device will be characterized cryogenically and magnetically prior to its installation next year on the APS storage ring.

#### ACKNOWLEDGMENTS

The authors would like to thank to Kurt Boerste, Susan Bettenhausen, John TerHAAR and Jason Ackley from APS's Magnetic Devices Group for the technical support; to John Andrist from APS's AES-DD for designing the cryostat subcomponents; to Steven T. Krave and Sean M. Johnson from FNAL's Technical Division for laser ablation of the mica insulations; and to Elpidio Garcia from FNAL's Technical Division for helping to prepare the magnets and short samples for reactions; to V. Marinozzi from FNAL's Technical Division and C. Kovacs from Ohio State University for the HiPot tests. The authors also would like to thank Kathleen Edwards, Lucas Brouwer, and Reed Teyber from LBNL for quench simulations that helped the design of the protection system; and to Marcos Turqueti and Jordan Taylor from LBNL for fabrication and installation of the quench detection and protection system.



## REFERENCES

- [1] A. V. Zlobin, E. Barzi, D. Turrinoni, Y. Ivanyushenkov, and I. Kesgin, "Advantage and Challenges of Nb<sub>3</sub>Sn Superconducting Undulators," presented at the 9th International Particle Accelerator Conference, Vancouver, BC, Canada, 04/29-05/04/2018, 2018. [Online]. Available: <https://www.osti.gov/servlets/purl/1437282>.
- [2] H. W. Weijers, K. R. Cantrell, A. V. Gavrilin, and J. R. Miller, "A Short-Period High-Field Nb<sub>3</sub>Sn Undulator Study," *IEEE Transactions on Applied Superconductivity*, vol. 16, no. 2, pp. 311-314, 2006, doi: 10.1109/TASC.2006.870783.
- [3] H. W. Weijers, K. R. Cantrell, A. V. Gavrilin, E. L. Marks, and J. R. Miller, "Assembly Procedures for a Nb<sub>3</sub>Sn Undulator Demonstration Magnet," *IEEE Transactions on Applied Superconductivity*, vol. 17, no. 2, pp. 1239-1242, 2007, doi: 10.1109/TASC.2007.899988.
- [4] S. Prestemon *et al.*, "Design and evaluation of a short period Nb<sub>3</sub>Sn superconducting undulator prototype," in *Particle Accelerator Conference, 2003. PAC 2003. Proceedings of the*, 12-16 May 2003 2003, vol. 2, pp. 1032-1034 Vol.2, doi: 10.1109/PAC.2003.1289595.
- [5] S. H. Kim, C. L. Doose, R. L. Kustom, and E. R. Moog, "Development of Short-Period Nb<sub>3</sub>Sn Superconducting Undulators for the APS," *IEEE Transactions on Applied Superconductivity*, vol. 18, no. 2, pp. 431-434, 2008, doi: 10.1109/TASC.2008.920528.
- [6] D. R. Dietderich *et al.*, "Fabrication of a Short-Period Nb<sub>3</sub>Sn Superconducting Undulator," *IEEE Transactions on Applied Superconductivity*, vol. 17, no. 2, pp. 1243-1246, 2007, doi: 10.1109/TASC.2007.897747.
- [7] I. Kesgin *et al.*, "Development of Short-Period Nb<sub>3</sub>Sn Superconducting Planar Undulators," *IEEE Transactions on Applied Superconductivity*, vol. 29, no. 5, pp. 1-4, 2019, doi: 10.1109/TASC.2019.2897645.
- [8] I. Kesgin *et al.*, "Fabrication and Testing of 10-Pole Short-Period Nb<sub>3</sub>Sn Superconducting Undulator Magnets," *IEEE Transactions on Applied Superconductivity*, vol. 30, no. 4, pp. 1-5, 2020, doi: 10.1109/TASC.2020.2964193.
- [9] Y. Ivanyushenkov *et al.*, "Status of the Development of Superconducting Undulators at the Advanced Photon Source," *Synchrotron Radiation News*, vol. 31, no. 3, pp. 29-34, 2018/05/04 2018, doi: 10.1080/08940886.2018.1460172.
- [10] Y. Ivanyushenkov *et al.*, "Development and operating experience of a short-period superconducting undulator at the Advanced Photon Source," *Physical Review Special Topics - Accelerators and Beams*, vol. 18, no. 4, p. 040703, 04/29/ 2015, doi: 10.1103/PhysRevSTAB.18.040703.
- [11] Y. Ivanyushenkov *et al.*, "Development and operating experience of a 1.1-m-long superconducting undulator at the Advanced Photon Source," *Physical Review Accelerators and Beams*, vol. 20, no. 10, p. 100701, 10/03/ 2017, doi: 10.1103/PhysRevAccelBeams.20.100701.
- [12] M. Kasa *et al.*, "Development and operating experience of a 1.2-m long helical superconducting undulator at the Argonne Advanced Photon Source," *Physical Review Accelerators and Beams*, vol. 23, no. 5, p. 050701, 05/18/ 2020, doi: 10.1103/PhysRevAccelBeams.23.050701.
- [13] I. Kesgin, Q. Hasse, Y. Ivanyushenkov, and U. Welp, "Performance of 2G-HTS REBCO Undulator Coils Impregnated Epoxies Mixed With Different Fillers," *IEEE Transactions on Applied Superconductivity*, vol. 27, no. 4, pp. 1-4, 2017, doi: 10.1109/TASC.2016.2638431.
- [14] E. Barzi, M. Kasa, I. Kesgin, D. Turrioni, and A. V. Zlobin, "Heat threatment studies of Nb<sub>3</sub>Sn wire for supeconducting planar undulators," *IEEE Transactions on Applied Superconductivity*, vol. Submitted, 2020.